Journal of Hydrology (2007) **339**, 29–38

available at www.sciencedirect.com

ScienceDirect

journal homepage: www.elsevier.com/locate/jhydrol

Analytical solution and analysis of solute transport in rivers affected by diffusive transfer in the hyporheic zone

F. De Smedt *

Department of Hydrology and Water Resources Engineering, Vrije Universiteit Brussel, Belgium

Received 6 November 2006; received in revised form 31 January 2007; accepted 2 February 2007

KEYWORDS
Solute transport;
Analytical solution;
Tracer experiment;
Hyporheic zone

Summary A model is presented for solute transport in rivers including transient storage in hyporheic zones. The model consists of an advection–dispersion equation for transport in the main channel with a sink term describing diffusive solute transfer to the hyporheic zone. This system of equations is solved analytically for instantaneous injection of a conservative tracer in an infinite uniform river reach with steady flow. The solution enables to estimate the temporal and spatial evolution of tracer concentrations downstream of the injection point with fewer parameters than any other model before. The solution is linked to a non-linear least squares optimisation algorithm to analyse breakthrough curves and estimate solute transport parameters. The model is applied to tracer experiments conducted in the Chillán River, Chile, which were previously analysed with a model including mass exchange between the river and a stagnant storage zone. The fit between observations and model results is good, except for some experiments where the tailing of the fitted curves is more pronounced than observed. Estimates of the water flow velocity are practically identical with previous findings, but the estimates of the cross-sectional area and the dispersion coefficient are markedly different. Estimated values for the diffusion coefficient in the hyporheic zone agree with values cited in literature and with the magnitude of chemical diffusion coefficients in porous media.
© 2007 Elsevier B.V. All rights reserved.

Introduction

Numerous tracer experiments have shown that transport of dissolved chemicals in rivers and streams is affected by retention of the solutes in transient storage zones (e.g. Bencala and Walters, 1983; Bencala, 1984; Legrand-Marq and Laudelout, 1985; Harvey et al., 1996; Morrice et al., 1997; Harvey and Fuller, 1998; Czernuszenko et al., 1998; Fernald et al., 2001; van Mazijk and Veling, 2005; see also the references cited by Runkel et al., 2003). Transient storage occurs

* Tel.: +32 2 629 3547; fax: +32 2 629 3022.
E-mail address: fdesmedt@vub.ac.bez

0022-1694/$ - see front matter © 2007 Elsevier B.V. All rights reserved.
doi:10.1016/j.jhydrol.2007.02.002

when water and dissolved chemicals become temporarily isolated from the main channel in stagnant water zones, such as pools, dead-end side channels, or adjacent wetland areas. In addition, significant portions of the water and dissolved chemicals may interchange with the hyporheic zone, i.e. porous banks and bed sediments near and under a stream or river where groundwater and surface water mix. Typical effects of this interchange are retardation of solute migration and a skewed shape of solute concentration profiles in the main stream channel that cannot be explained by classical advection–dispersion theory (Day, 1975; Chatwin, 1980; Nordin and Troutman, 1980; van Mazijk and Veling, 2005).

Several models have been formulated to explain solute transport in rivers with mass exchange in stagnant water zones. The most widespread approach considers a one-dimensional advection–dispersion equation in combination with first-order mass exchange between the river and a lumped stagnant storage zone, with a mass exchange flux assumed to be proportional to the difference in solute concentration between the river and the stagnant storage zone (Hays et al., 1966; Nordin and Troutman, 1980; Bencala and Walters, 1983; Legrand-Marq and Laudelout, 1985; Bencala et al., 1990; Czernuszenko and Rowinski, 1997; Choi et al., 2000). The resulting effect of the transient storage depends upon two parameters, i.e. a mass exchange rate coefficient and the volume or cross-sectional area of the transient storage zone (Runkel et al., 2003). Analytical solutions for this model have been presented by Hart (1995), Davis et al. (2000), De Smedt et al. (2005), and De Smedt (2006). For a summary of status and scope of transient storage model development and application see Bencala (2005).

Other approximate solutions are based on the analysis of the temporal moments of concentration profiles in the main channel (Hays et al., 1966; Nordin and Troutman, 1980; Schmid, 1995; Runkel, 1996; Czernuszenko and Rowinski, 1997; Schmid, 2003). Some investigators proposed similarity functions that have the same temporal moments as the observed concentration profiles (Liu and Cheng, 1980; Chatwin, 1980; Schmid, 1995; van Mazijk and Veling, 2005). Also very much used in practice is an approximate finite difference solution (Runkel and Chapra, 1993), which forms the basis of the numerical one-dimensional transport with inflow and storage (OTIS) model (Runkel and Chapra, 1993; http://co.water.usgs.gov/otis). This model was extended with a parameter optimisation technique, OTIS-P (Runkel, 1998), and has been used extensively for analysing tracer experiments to estimate transient storage characteristics in rivers (e.g. Choi et al., 2000; Lees et al., 2000; Fernald et al., 2001; Laenen and Bencala, 2001; Keefe et al., 2004).

Other approaches are less popular. Jackman et al. (1984) introduced a model consisting of a one-dimensional advection–dispersion equation in the river linked to lateral solute diffusion in the hyporheic zone. The resulting transport equations were solved numerically. Comparison with the first-order mass exchange approach showed that the diffusion model is somewhat more complicated from computational point of view but performs better in predicting observed solute concentration profiles. Wörman (1998) gave an analytical solution for this model in case dispersion in the river is neglected and the hyporheic zone is infinite in extend. The solution was successfully applied to interpret the transport of solutes in several tracer experiments. Wörman (2000) showed that the first-order mass exchange approach and the diffusion approach yield similar representations of the first three temporal moments of solute concentration profiles in the river. In this study, dispersion in the river was also neglected, but the hyporheic zone was assumed either finite, or as an alternative infinite with in addition to diffusion also advective transport from the hyporheic zone to the river.

A new approach is based on describing the residence time distribution of the solutes in the hyporheic zone. Wörman et al. (2002) proposed a log normal distribution as an approximation of residence times resulting from solute advection along hyporheic flow paths induced by water pressure differences over a permeable bed. Gooseff et al. (2003) proposed a power law residence time distribution, instead of an exponential relation. However, these empirical approaches do not enable to obtain any physical insight in the governing processes.

The purpose of this study is to extend the modelling approach of Wörman (1998), i.e. diffusion of solute into an infinite hyporheic zone, by including dispersion in the river, and to derive an appropriate analytical solution for instantaneous injection of a tracer in a river and show how this solution can be used in practice to predict transport of dissolved chemicals and observed concentration profiles.

Theory

Transport of solutes in streams with transient storage is modelled following the approach presented by Wörman (1998), but including dispersion in the river. Consider a uniform stream channel with a cross-sectional area A [L^2], as schematically depicted in Fig. 1. The water flow is assumed steady with a flow rate Q [L^3T^{-1}]. When a chemical is introduced in the stream dispersion will produce a cross-sectional average solute concentration $C(x,t)$ [ML^{-3}], where x is the longitudinal distance [L] in the main stream channel and t is the time [T]. Also, because of dispersion, the chemical is in continuous contact with the hyporheic zone, which enables diffusive interchange along the wetted perimeter L [L] of the river channel, as depicted in Fig. 1. Hence, the chemical diffuses in the hyporheic zone with a concentration $C_h(x,z,t)$ [ML^{-3}], where z [L] is the lateral distance measured from the river channel bed into the hyporheic zone. The resulting transport equation in the river is

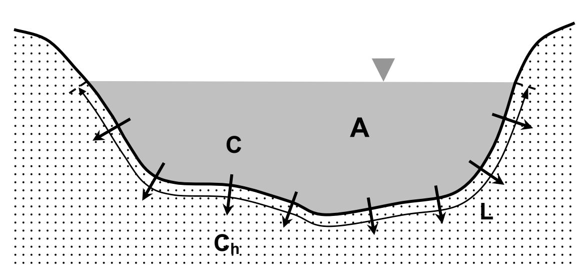

Figure 1 Schematic cross-section of a river channel and the hyporheic zone, showing the cross-sectional area A, the wetted perimeter P, and the solute concentrations C in the river and C_h in the hyporheic zone.

$$A\frac{\partial C}{\partial t} = AD\frac{\partial^2 C}{\partial x^2} - Q\frac{\partial C}{\partial x} + LD_h\frac{\partial C_h}{\partial z}\bigg|_{z=0}, \tag{1}$$

where D is the dispersion coefficient [L^2T^{-1}] in the river channel, and D_h is the diffusion coefficient [L^2T^{-1}] in the hyporheic zone. The last term on the right-hand side of Eq. (1) gives the diffusion flux of solute entering the hyporheic zone. Dividing by the cross-sectional area A, results in

$$\frac{\partial C}{\partial t} = D\frac{\partial^2 C}{\partial x^2} - v\frac{\partial C}{\partial x} + \frac{D_h}{R}\frac{\partial C_h}{\partial z}\bigg|_{z=0}, \tag{2}$$

where $v = Q/A$ is the cross-sectional averaged velocity [LT^{-1}] in the river, and $R = A/L$ is the hydraulic radius [L] of the river cross-section (which in practice can often be approximated by the average water depth in natural streams).

In a typical tracer experiment, a mass M [M] of tracer is injected at time zero and location $x = 0$, well mixed over the cross-sectional area A [L^2] of the main stream channel, so that the initial condition is given by

$$C(x,0) = (M/A)\delta(x), \tag{3}$$

where $\delta(x)$ is the Dirac function [L^{-1}]. In addition, it is assumed that there can never be any tracer at infinity

$$C(\pm\infty, t) = 0. \tag{4}$$

The distribution and transport of the solute in the hyporheic zone is described by a one-dimensional diffusion equation

$$\frac{\partial C_h}{\partial t} = D_h\frac{\partial^2 C_h}{\partial z^2}, \tag{5}$$

Initially, the hyporheic zone is free of solute

$$C_h(x,z,0) = 0, \tag{6}$$

and at the river bed, the solute concentrations in the river and the hyporheic zone are equal

$$C_h(x,0,t) = C(x,t). \tag{7}$$

For the boundary condition at the other extreme of the hyporheic zone, Jackman et al. (1984) assumed a hyporheic zone of limited extend with a zero flux condition, but here we will follow Wörman (1998) who assumed that the hyporheic zone is infinite; hence

$$C_h(x,\infty,t) = 0. \tag{8}$$

The solution of Eq. (2) subjected to conditions (3)–(8), is derived in Appendix A and is given by

$$C(x,t) = \int_0^t C_0(x,\tau)\frac{\tau}{2R}\sqrt{\frac{D_h}{\pi(t-\tau)^3}}\exp\left[-\frac{D_h\tau^2}{4R^2(t-\tau)}\right]d\tau, \tag{9}$$

where $C_0(x,t)$ is the solution of the classical advection–dispersion equation subjected to the same initial and boundary conditions

$$C_0(x,t) = \frac{M/A}{2\sqrt{\pi Dt}}\exp\left[-\frac{(x-vt)^2}{4Dt}\right]. \tag{10}$$

The link with the solution presented by Wörman (1998) is achieved follows. When the dispersion in the river is neglected and in case of continuous injection of tracer with a constant concentration C_i, the solution given by Eq. (9) remains valid, but with $C_0(x,t)$ given by

$$C_0(x,t) = C_iH(vt-x), \tag{11}$$

where H is the Heaviside function. When Eq. (11) is substituted in Eq. (9) it follows that

$$C(x,t) = C_iH(vt-x)erfc\left(\frac{x}{2Rv}\sqrt{\frac{D_h}{t-x/v}}\right), \tag{12}$$

where *erfc* is the co-error function. Eq. (12) is the solution given by Wörman (1998).

A similar expression as Eq. (9) has been presented by Maloszewski and Zuber (1990) for chemical transport in a single fissure in a porous matrix, for which the transport equations are similar as Eqs. (1) and (5) but the boundary conditions are different because the medium is considered semi-finite ($x \geqslant 0$) and the chemical is injected as an instantaneous slug input at the upper boundary, i.e. $C(0,t) = M\delta(t)/Q$. The solution presented by Maloszewski and Zuber (1990) is similar as Eq. (9) if C_0 is replaced by the appropriate solution for these boundary conditions.

Eq. (9) can more conveniently be evaluated as

$$C(x,t) = \sqrt{\frac{\alpha t}{\pi}}\int_0^1 C_0(x,\lambda t)\frac{\lambda}{(1-\lambda)^{3/2}}\exp\left(-\frac{\alpha t\lambda^2}{1-\lambda}\right)d\lambda, \tag{13}$$

where α is a parameter with dimension [T^{-1}] given by

$$\alpha = D_h/4R^2, \tag{14}$$

which represents the influence of the solute exchange and storage in the hyporheic zone on the concentration profile in the river. From Eq. (13) it follows that the solute transfer in the hyporheic zone only depends upon α, while in the first-order mass exchange model two parameters are needed: the mass exchange coefficient and the size of the stagnant water zone. Hence, the present model is more parsimonious, which is a desirable model quality, but it remains to be proven whether the model is able to predict accurately observed tracer concentration profiles.

In order to illustrate the analytical solution, we assume an artificial situation where 1 kg of solute is instantaneously injected in the main channel of a river with a cross-section of 10 m^2, an average flow velocity of 1 m/s, and a dispersion coefficient of 5 m^2/s. We use different values for the exchange coefficient α, respectively, 0, $1\times10^{-6}\,s^{-1}$, $1\times10^{-5}\,s^{-1}$, and $1\times10^{-4}\,s^{-1}$, which are in the range of typical values as will be discussed further on. The concentrations in the main channel will be calculated at a distance of 1000 m downstream from the injection point. For the evaluation of the analytical solution, the convolution integral in Eq. (13) is calculated with the trapezium rule using 10,000 intervals. The results are given in Fig. 2. When α is zero, the analytical solution reduces to Eq. (10); notice that the integrand in Eq. (13) becomes $C_0\,(x,\lambda t)\delta(\lambda-1)$. When α is different from zero, the concentration curves show a pronounced tailing, which is a typical effect of diffusion in the hyporheic zone. However, unlike the first order exchange model, the tailing becomes more and more pronounced with increasing values of α. This is unlike the first order exchange model with a finite dead zone volume, where for large values of the exchange coefficient the concentration in the transient storage zone becomes indistinguishable from the concentration in the river because of the intense mixing

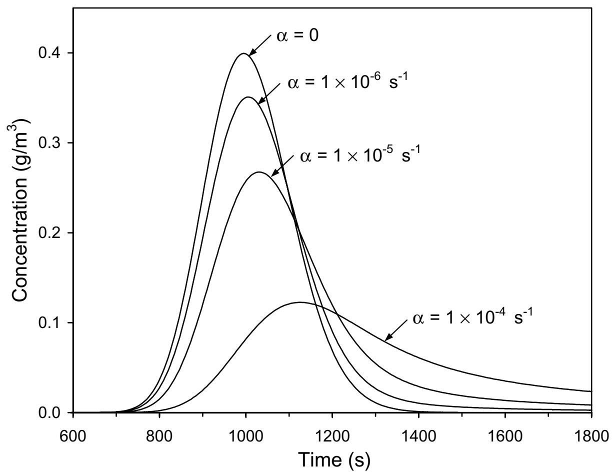

Figure 2 Typical concentration profiles calculated with the analytical solution for a hypothetical tracer experiment, considering 1 kg of solute instantaneously injected in the main channel of a river with a cross-section of 10 m^2, an average flow velocity of 1 m/s, a dispersion coefficient of 5 m^2/s, a ratio of storage zone and main channel cross-sectional area of 0.2, and different values for the transfer coefficient as indicated in the figure.

and short residence time. This phenomenon does not occur with the present model.

Application of the model

The usefulness of the analytical solution is demonstrated with a practical application involving the analysis of tracer experiments. In order to analyse breakthrough curves, resulting from instantaneous injection of a conservative tracer, the analytical solution is linked to a non-linear least squares optimisation algorithm (Marquardt, 1963), so that transport parameters that give the best match between observed and simulated concentration values can be estimated. A theoretical concentration profile can be fitted to an observed tracer breakthrough curve obtained at a certain sampling location, provided two experimental parameters are given, i.e. the injected mass M and the distance x between injection point and sampling location. The theoretical solution, given by Eq. (13), contains four parameters that can be optimised: the main channel cross-sectional area A, the flow velocity v, the dispersion coefficient D, and the exchange coefficient α.

The model is applied to tracer experiments conducted in the Chillán River, Chile, which were also analysed by De Smedt et al. (2005) with a one-dimensional advection–dispersion equation in combination with first-order mass exchange between the river and stagnant storage zones. A description of the Chillán river basin and the conducted tracer experiments can be found in Brevis et al. (2001a,b) and De Smedt et al. (2005). The experiments were conducted during the Austral summer of 2000–2001, when river discharge and water depths were low. Five tracer experiments were conducted using Rhodamine injected at two different locations, and breakthrough curves were measured at different sampling locations, denoted by numbers 1–10, at distances several 100–1000 m away from the injection sites, as shown in Fig. 3.

The tracer experiments are listed in Table 1, labelled with a code composed of a Roman number representing the experiment and an Arabic number representing the sampling location, similar as in De Smedt et al. (2005) for easy comparison. In addition, observed parameter are listed in Table 1, i.e. injected tracer mass M, longitudinal distance along the river course between injection and sampling location x, and observed average water depth at the sampling location which we will use as a substitute for the hydraulic radius R. At some locations the water depth was not measured and here the hydraulic radius, denoted by R^*, is estimated as will be explained later on. Experiments I, II and V where conducted using injection site 1, while for experiments III and IV injection site 2 was used.

Losses of Rhodamine WT during the tracer experiments are ignored in the analysis because of the short duration of the experiments. The results from the optimisation procedure are presented in the remaining columns of Table 1, giving the optimised values of the model parameters together with their 95% confidence intervals. Also, values of the river discharge $Q = vA$ are given, as computed from the optimised values of the velocity v and the cross-sectional area A. Notice that all these values should be considered as averages over the total river stretch from the injection point to the sampling location.

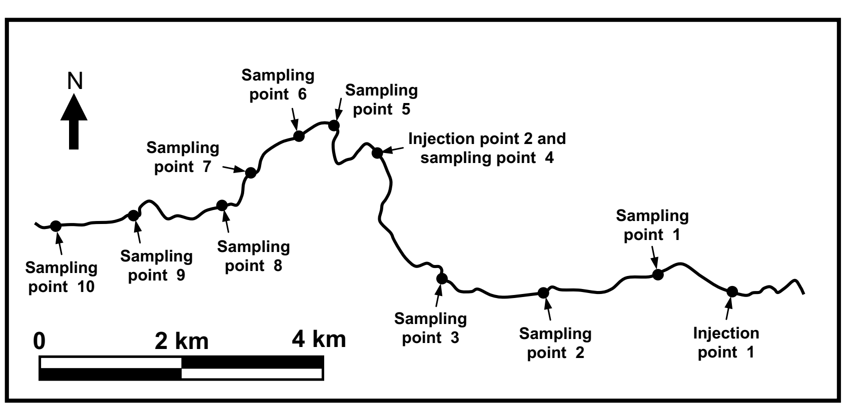

Figure 3 Setting of the tracer experiments conducted in the Chillán River, Chile.

Table 1 Observed and optimised parameter values with 95% confidence intervals for the tracer experiments

Exp.	M (g)	x (m)	R (m)	A (m^2)	v (m/s)	Q (m^3/s)	D (m^2/s)	α (10^{-5} s^{-1})	D_h (10^{-6} m^2/s)
I-3	157.1	4604	0.45[a]	14.1 ± 1.2	0.458 ± 0.006	6.46	7.05 ± 1.03	0.236 ± 0.091	1.945 ± 0.747
I-4	157.1	6524	0.48	17.6 ± 2.1	0.400 ± 0.001	7.04	5.88 ± 1.40	0.077 ± 0.054	0.722 ± 0.504
I-9	157.1	11646	0.59	15.3 ± 1.3	0.391 ± 0.004	5.98	6.33 ± 1.16	0.127 ± 0.037	1.759 ± 0.507
II-1	23.8	1100	0.23[a]	6.3 ± 0.9	0.196 ± 0.007	1.23	2.02 ± 0.51	0.112 ± 0.062	0.236 ± 0.129
II-2	23.8	2915	0.35	8.3 ± 0.7	0.168 ± 0.003	1.39	2.99 ± 0.37	0.164 ± 0.065	0.787 ± 0.314
II-3	23.8	4604	0.27[a]	7.5 ± 0.7	0.177 ± 0.003	1.33	3.88 ± 0.52	0.154 ± 0.055	0.434 ± 0.155
II-4	23.8	6524	0.32	7.4 ± 0.5	0.175 ± 0.002	1.30	3.70 ± 0.41	0.084 ± 0.024	0.343 ± 0.098
III-7	35.7	2969	0.24[a]	6.5 ± 0.4	0.187 ± 0.003	1.22	3.00 ± 0.53	0.540 ± 0.118	1.197 ± 0.260
III-10	35.7	6354	0.19	5.3 ± 0.5	0.187 ± 0.004	0.99	2.80 ± 0.81	0.463 ± 0.108	0.654 ± 0.152
IV-5	38.1	1594	0.20	5.9 ± 0.4	0.091 ± 0.002	0.54	1.04 ± 0.14	0.700 ± 0.145	1.076 ± 0.223
IV-6	38.1	1971	0.25	10.1 ± 0.5	0.098 ± 0.001	0.99	1.46 ± 0.13	0.633 ± 0.090	1.581 ± 0.225
IV-7	38.1	2969	0.33	9.3 ± 0.4	0.110 ± 0.001	1.02	1.97 ± 0.16	0.462 ± 0.060	1.954 ± 0.254
V-1	20.3	1100	0.19[a]	5.2 ± 0.6	0.131 ± 0.004	0.68	1.23 ± 0.30	1.008 ± 0.408	1.529 ± 0.618
V-2	20.3	2915	0.16[a]	4.1 ± 1.0	0.110 ± 0.006	0.45	1.62 ± 0.49	0.925 ± 0.435	0.938 ± 0.441

M: injected tracer mass, *x*: longitudinal distance along the river channel between injection and sampling location, *R*: hydraulic radius or average water depth at the sampling location, *A*: cross-sectional area of the river, *v*: cross-sectional averaged water flow velocity, *Q*: calculated river discharge, *D*: cross-sectional averaged longitudinal dispersion coefficient in the river, and α: exchange coefficient between the river and the hyporheic zone; the last column gives values of the diffusion coefficient in the hyporheic zone D_h calculated from the mass exchange coefficient α and the hydraulic radius *R* with Eq. (14).

[a] Estimated.

Results and discussion

The results of the model optimisation for the first tracer experiment I are shown in Fig. 4, depicting observed and fitted concentration profiles versus time at different measurement locations. The fit between observations and simulations is good, although one can notice somewhat more pronounced tailing of the fitted curves compared to the observations, especially for the first two experiments I-3 and I-4. The measured and fitted concentration curves show typical shapes and trends, with peak values decreasing at consecutive sampling locations, while the solute plume is increasingly spreading out due to dispersion in the river. Also, the tailing of the breakthrough curves is prominent due to the diffusion in and out of the hyporheic zone.

Parameters *A* and *v* are rather accurately estimated which is reflected by their small confidence intervals, while this is not the case for *D* and α (Table 1). The estimated values for the cross-sectional area and the flow velocity are fairly constant, which confirms the assumption of constant flow used in the transport equations (Eq. (1)). The dispersion coefficient *D* and exchange coefficient α are less uniform over the different sections, but nevertheless the values are in the same order of magnitude and are close enough to be consistent. Remarkable is that the confidence limits are rather large, which indicates that these parameters are much more insecure, and cannot be accurately fitted from the observed data. The reason for the less accurate estimation of parameters *D* and α is probably due to the fact both parameters represent processes that produce spreading and tailing of the dissolved tracer in the river; hence, parameters *D* and α are correlated, which is an undesirable property for accurate estimation. Remarkable is also that although the measurements at the last sampling point were interrupted too early, this has little effect on the confidence interval of parameter α compared to the previous sampling points.

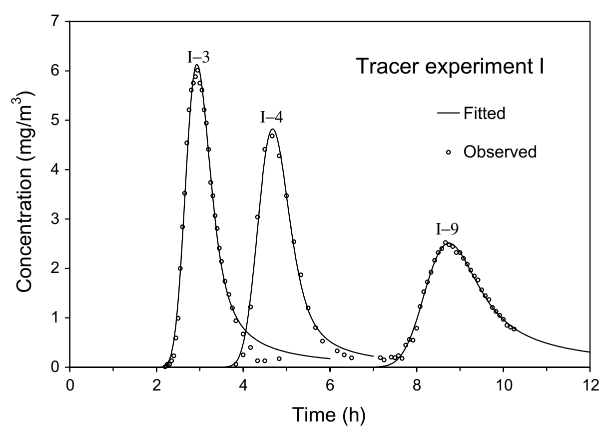

Figure 4 Fitted and observed concentrations for the first tracer experiment. Observations are shown by open dots and simulated curves by solid lines, calculated with the optimised parameter values given in Table 1.

The resulting breakthrough curves for the second experiment are shown in Fig. 5. This was the largest experiment conducted as breakthrough concentration profiles were measured at four locations. The fit between theoretical concentration profiles and field observations is good, but again the theoretical curves show somewhat more tailing. From the optimised parameter values presented in Table 1, one can notice that *A* and *v* are nearly constant along the river reach, while there is more variation for the other parameters *D* and α. The values of the dispersion coefficient seem to increase along the river stretch, while there is no clear trend in the estimated values of exchange coefficient α. In previous study (De Smedt et al., 2005), where the observations were fitted with a first-order mass exchange model, it was concluded that in the last part of the river

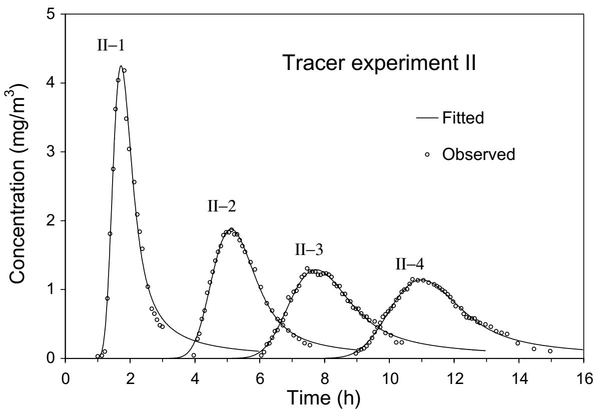

Figure 5 Fitted and observed concentrations for the second tracer experiment. Observations are shown by open dots and simulated curves by solid lines, calculated with the optimised parameter values given in Table 1.

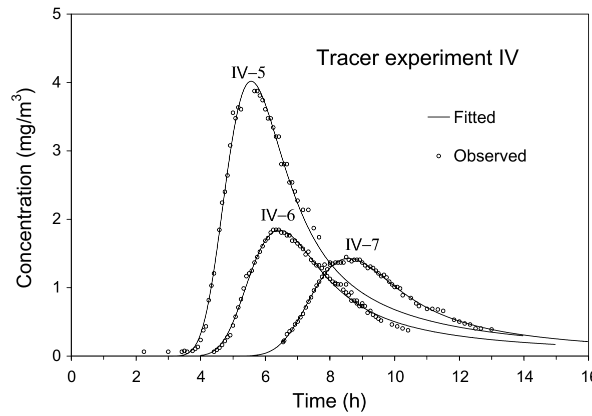

Figure 7 Fitted and observed concentrations for the fourth tracer experiment. Observations are shown by open dots and simulated curves by solid lines, calculated with the optimised parameter values given in Table 1.

there is much less transient storage than in the upper part, which could be explained by the fact that upstream of sampling point 2 the bed of the Chillán River is made up mainly of cobble and gravel, while downstream of this point the river frequently cuts through bedrock. The present findings agree partly with this, because there is a marked decrease in the value α for the last section. As the estimated values should be considered as averages over the total river stretch from injection to sampling point, this indicates that there is reduced diffusion in the hyporheic zone in the last section of the river probably due to impervious bedrock. Also notice that estimated values for D and α are very similar to what was obtained for the first tracer experiment.

The results for the third tracer experiment are shown in Fig. 6. Unfortunately the measurements are incomplete and appear to be somewhat irregular, even showing two peaks in the second curve. However, all model parameters are estimated rather accurately with small confidence limits. In addition, there is almost no difference between estimated parameter values at the two sampling locations. Also, the results are in line with the previous experiments, except that there is a marked increase in the value of the exchange coefficient α, for which no obvious explanation can be given, unless the incompleteness of the data series and the shallow water depth that was observed at sampling point 10.

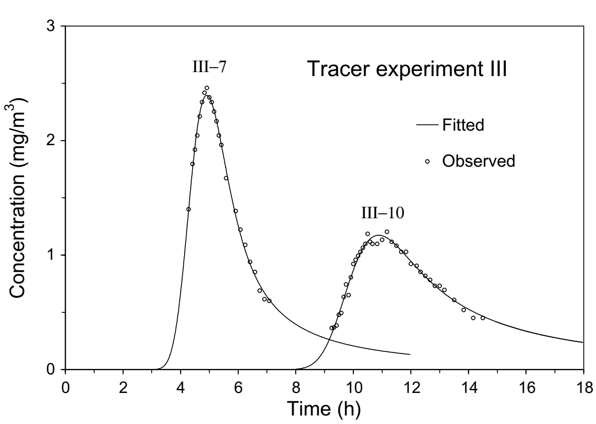

Figure 6 Fitted and observed concentrations for the third tracer experiment. Observations are shown by open dots and simulated curves by solid lines, calculated with the optimised parameter values given in Table 1.

Results of the fourth tracer experiment are given in Fig. 7. The marked decrease in concentration values between sampling point 5 and sampling points 6 and 7 is due to a tributary entering the Chillán River just downstream of sampling point 5, which obviously dilutes the tracer concentration considerably. Nevertheless, all observed concentration curves can be well fitted with the theoretical model. The fact that the tributary brings in a lot of water is also reflected in the sudden increase in the fitted values for the cross-sectional area A, which almost doubles between sampling location 5 and locations 6 and 7. As the flow velocity remains almost constant throughout the different sections, we can conclude that there is a strong increase in river discharge between sampling stations 5 and 6 due to the confluence. It is also noticed that he fitted values of the dispersion coefficient D are smaller than what was obtained for the previous experiments. This is likely due do the very small flow velocities that occurred during this experiment, as will be explained further on. On the other hand, the fitted values for exchange coefficient α are larger than what was obtained for the previous experiments. Again this could be due to the very shallow water depths that were observed at all sampling stations. We will also elaborate on this further on.

The results for the fifth experiment are shown in Fig. 8. Unfortunately, the measurements in sampling station 2 were stopped premature. The fit between theoretical and observed breakthrough curves is good, although somewhat more tailing can be noticed in the first theoretical curve V-1 compared to the observations. Again the fitted values for the dispersion coefficient D are small and the exchange coefficient α is distinctively larger compared to other experiments. There are no observations of the water depth available for this experiment, but from the small cross-sectional areas and the very small water flow velocities it can inferred that the river must have been very shallow.

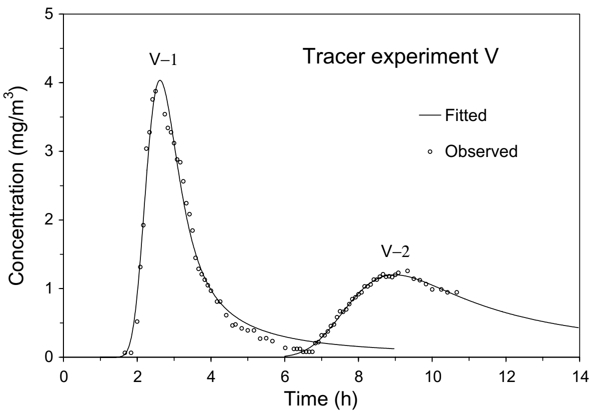

Figure 8 Fitted and observed concentrations for the fifth tracer experiment. Observations are shown by open dots and simulated curves by solid lines, calculated with the optimised parameter values given in Table 1.

Although the assumption of uniform flow and constant transport parameters cannot be expected to hold over large distances, reasonably good results have been obtained with the model for all tracer experiments. When we compare these results with the approach based on the model with first-order mass exchange to a stagnant storage zone (De Smedt et al., 2005) some striking similarities and differences become evident. First of all, the fitting of the observed breakthrough curves is somewhat better with the first-order mass exchange model compared to the present results. This should be no surprise as the first-order mass exchange model has five parameters that can be adjusted to optimise the fit between the model and the observations. This is also reflected in the resulting sum of squares of the residuals, which are close for both models, except for some notable exceptions where the first-order mass exchange model performs better. These are especially experiments I-3, I-4, IV-6, and V-1, for which the present model predicts somewhat more tailing of the breakthrough curves compared to the observations. It also follows that the parameters of the first-order mass exchange model are more accurately estimated, resulting in smaller confidence limits.

Comparing values of common parameters in both models, it follows that estimates of the water flow velocity are practically identical, while those of the cross-sectional area and the dispersion coefficient are markedly different. This shows that the velocity is largely determined by the appearance of the leading edge and especially the peak of the breakthrough curve and does not much depend on the tail or how we conceptualise the model to explain the tailing of the breakthrough curves. For the cross-sectional area, the values obtained with the present model are consistently and substantially lower than for the first-order mass exchange model. Probably this must be due to the mass balance that has to be respected in both models as decay of the tracer is ignored. Mass balance requires the following equality

$$M = vA \int_0^\infty C\,dt. \qquad (15)$$

Because the velocities are the same, but the integral of the concentrations is larger in the present model due to the pronounced tailing, the estimated cross-sectional area has to compensate for this to respect the mass balance, and, hence, has to be smaller. As a consequence, if the tracer experiments would have been conducted for determining the river discharge $Q = vA$, the differences between the two models would be considerable. Hence, the model concept has a large influence on the estimation of the river discharge. For instance, for experiment I-3 the river discharge estimated with the present model is 6.46 m^3/s while this is 8.68 m^3/s for the first-order mass exchange model.

The dispersion coefficients in the river channel estimated with the present model are mostly larger, sometimes as much as doubled, compared to the values obtained with the first-order mass exchange model. Again the differences become larger for experiments that are fitted with a theoretical curve showing pronounced tailing, as for experiments I-3, I-4, and V-1. It is not immediately clear what could be the reason for this.

We now discuss some overall characteristics of the results obtained with the present model. We already explained that the value of the water flow velocity v depends primarily on the time instance of the occurrence of the peak of the breakthrough curve, while the value of the cross-sectional area A follows from fitting the mass balance. The dispersion coefficient depends upon the friction velocity and dimensions of the river channel, as expressed by Fischer et al. (1979). For uniform flow the friction velocity can be related to the average flow velocity which implies that the dispersion coefficient should increase more or less linearly with the average flow velocity, ignoring secondary effects of changes in water level, river width, and flow resistance. Fig. 9 depicts all combined estimated dispersion coefficients versus flow velocities in the Chillán River. Hereby we have assumed that all cross-sections have similar characteristics and, hence, all data can be combined as if belonging to the same location. Although there is some scatter in de data due to uncertainty in the estimated values,

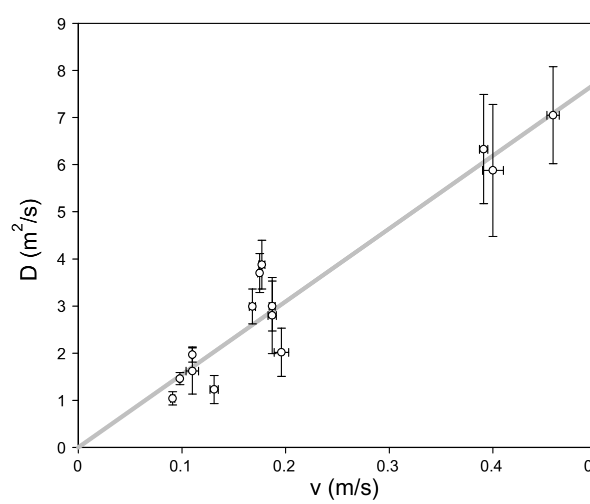

Figure 9 Estimated values with 95% confidence intervals of the dispersion coefficient D versus the river flow velocity v; the solid line gives the best least square regression fitted line forced through the origin.

especially of the dispersion coefficient, and the data points belong to different locations, a more or less linear relationship between dispersion coefficient and flow velocity seems reasonable, as shown by the straight line forced through the origin and fitted through the data points. Hence, this complies with the theory of Fischer et al. (1979). However, when compared to similar results obtained with the stagnant storage zone model results of De Smedt et al. (2005), the present linear relationship between dispersion coefficient and flow velocity is much more evident, while the slope of the linear relationship is practically the same. In particular, also the dispersion coefficient versus flow velocity for experiments I-3, I-4, and V-1 very well fit the linear relationship as for the other experiments, although the present model predicts more tailing than what is observed. On the other hand, with the stagnant storage zone model much lower values were estimated for the dispersion coefficient for these experiments, which deviated considerably from the linear relationship that was present in the other experiments. Hence, although the present model seems to perform less for these experiments, the obtained parameter values are more in line with the rest of the experiments, which was not the case with the stagnant storage zone model (De Smedt et al., 2005).

Estimated values of the exchange coefficient α versus water flow velocity v are presented in Fig. 10, together with their 95% confidence intervals. The α-values vary between zero and about $1 \times 10^{-5}\ s^{-1}$, and seem to decrease with increasing water flow velocity. However, we should keep in mind that α is a variable derived from the diffusion coefficient in the hyporheic zone D_h and the hydraulic radius of the river channel R, as given by Eq. (14). From Table 1 it follows that there were differences in hydraulic radius between the experiments. For the experiments where the hydraulic radius was measured (actually the average water depth in the river), the corresponding values of D_h can be interfered from the α-values by inverting Eq. (14). For the experiments where the hydraulic radius was not measured, the hydraulic radius was estimated using a non-linear regression between observed values of the hydraulic radius

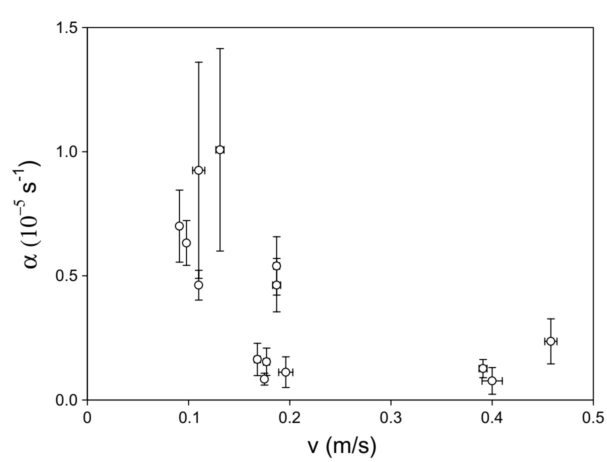

Figure 10 Estimated values with 95% confidence intervals of the exchange coefficient α versus the average main channel flow velocity v.

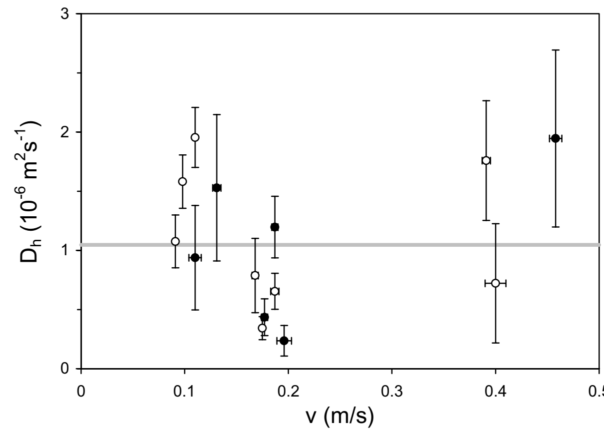

Figure 11 Estimated values with 95% confidence intervals of the diffusion coefficient in the hyporheic zone D_h versus the river flow velocity v; open dots are D_h-values obtained from observed hydraulic radius R, while the closed dots are values obtained from estimated R^*-values; the solid curve represents the un-weighted mean value of the diffusion coefficient in the hyporheic zone D_h.

and corresponding estimated values of the cross-sectional area, i.e. $R \approx 0.048A^{0.85}$, with a correlation coefficient 0.79; these are the R^a-values listed in Table 1. Consequently, also values for D_h can be estimated for these experiments, though less precise. The obtained values for D_h for all experiments are given in the last column of Table 1. These values are also plotted versus v in Fig. 11, and show no particular trend. The D_h-values vary between zero and $2 \times 10^{-6}\ m^2/s$, with an average $1.05 \times 10^{-6}\ m^2/s$, which fits within most of the estimated 95% confidence limits of all experiments. There are no values of the diffusion coefficient in the hyporheic zone cited in the literature, except for the paper of Wörman (1998), who on the basis of Cr transport in the Vistula River, Poland, and a tentative analysis of Chernobyl Cs transport in several European rivers, concluded that D_h was found to vary within the range of 0.1×10^{-6}–$10 \times 10^{-6}\ m^2/s$. Hence, this complies with the present results. Furthermore, the range of values found in this study also agrees with what one could expect as order of magnitude of the diffusion coefficient of inert chemicals in a porous medium as a river bed.

Conclusions

A model has been proposed for solute transport in rivers and streams affected by exchange with the hyporheic zone. The hyporheic zone is assumed to be infinite in extend and the solute exchange between river and hyporheic zone to be governed by diffusion only. This model proves to be very parsimony with respect to considered physical processes and essential parameters compared to any other theory. The resulting transport equation for dissolved chemicals in a river is solved analytically for the case of an instant injection of a tracer mass in a river section with uniform flow. The solution enables to predict the temporal and spatial evolution of the tracer concentration downstream of an injection point.

The solution is linked to a non-linear least squares optimisation algorithm, in order to estimate solute transport parameters from observed breakthrough curves, which allow to estimate the flow velocity, cross-sectional area, and dispersion coefficient in the river channel, and the exchange coefficient between the river and the hyporheic zone. The latter is a secondary variable derived from the hydraulic radius of the river and the diffusion coefficient in the hyporheic zone.

The optimisation procedure is successfully applied to interpret tracer experiments conducted in the Chillán River, Chile, which were previously analysed with a first-order mass exchange between river and a stagnant storage zone model by De Smedt et al. (2005). The fit between observations and model results is good, although for some experiments the tailing of the fitted curves is somewhat more pronounced compared to the observations.

Comparing values of common parameters in both models, it follows that estimates of the water flow velocity are practically identical, while those of the cross-sectional area and the dispersion coefficient are markedly different. This shows that the velocity is largely determined by the leading edge and especially the peak of the breakthrough curve and does not much depend on the tail. Values obtained for the cross-sectional area of the river channel are substantially lower compared to the first-order mass exchange model, which also leads to considerable differences in the estimated river discharge. Dispersion coefficients in the stream channel estimated with the present model are mostly larger compared to the values obtained with the first-order mass exchange model, but better fit a linear relationship with the flow velocity.

Estimated values for the diffusion coefficient in the hyporheic zone vary between zero and $2\times10^{-6}\,\mathrm{m^2/s}$, with an average of about $1.\times10^{-6}\,\mathrm{m^2/s}$, which corresponds with other values cited in the literature and the expected magnitude of chemical diffusion coefficients in porous media.

It can be concluded that the presented analytical solution for solute transport in rivers affected by diffusive exchange with an infinite hyporheic zone is a useful model for analysing tracer experiments and estimation of transport parameters.

Appendix 1. Derivation of the analytical solution

The solution is obtained by means of the Laplace transform. We denote the Laplace transform of a function $f(t)$ as

$$\bar{f}(s) = L[\mathrm{f}(t); t \to s] = \int_0^\infty f(t)\mathrm{e}^{-st}\,\mathrm{d}t. \tag{A1}$$

The Laplace transform of Eq. (2), taking into the initial condition Eq. (3), is

$$D\frac{\partial^2\overline{C}}{\partial x^2} - v\frac{\partial\overline{C}}{\partial x} - s\overline{C} + \frac{D_\mathrm{h}}{R}\frac{\partial\overline{C_\mathrm{h}}}{\partial z}\bigg|_{z=0} = -\frac{M}{A}\delta(x), \tag{A2}$$

and the Laplace transform of Eq. (5) with initial condition Eq. (6) is

$$D_\mathrm{h}\frac{\partial^2\overline{C_\mathrm{h}}}{\partial z^2} - s\overline{C_\mathrm{h}} = 0, \tag{A3}$$

Eq. (A3) can be solved taking into account Eqs. (7) and (8), to yield

$$\overline{C_\mathrm{h}} = \overline{C}\exp(-z\sqrt{s/D_\mathrm{h}}), \tag{A4}$$

which enables to calculate the diffusive flux into the hyporheic zones, using Eq. (7), as

$$\frac{D_\mathrm{h}}{R}\frac{\partial\overline{C_\mathrm{h}}}{\partial z}\bigg|_{z=0} = -\frac{\sqrt{sD_\mathrm{h}}}{R}\overline{C}. \tag{A5}$$

This can be substituted in Eq. (A2) yielding

$$D\frac{\partial^2\overline{C}}{\partial x^2} - v\frac{\partial\overline{C}}{\partial x} - \left(s + \frac{\sqrt{sD_\mathrm{h}}}{R}\right)\overline{C} = -\frac{M}{A}\delta(x), \tag{A6}$$

When D_h is zero, Eq. (A6) reduces to the classical advection–dispersion equation, with solution $C_0(x,t)$, hence

$$\overline{C}(x,s) = \overline{C_0}(x, s + \sqrt{sD_\mathrm{h}}/R). \tag{A7}$$

To obtain the inverse Laplace transform of Eq. (A7), we make use of the convolution theorem of the Laplace transform (Sneddon, 1974, p. 228)

$$L\left[\int_0^t f(\tau, t-\tau)\,\mathrm{d}\tau; t \to s\right] = L\{L[f(t_1,t_2); t_2 \to s]; t_1 \to s\}. \tag{A8}$$

Eq. (A7) is now written as

$$\overline{C}(x,s_1,s_2) = \overline{C_0}(x, s_1 + \sqrt{s_2D_\mathrm{h}}/R). \tag{A9}$$

where $s_1 = s_2 = s$, but different indexes are used to indicate that the inverse transformation is performed in two steps. The first inverse with respect to s_1 gives

$$L[C(x,t_1,t_2); t_2 \to s_2] = C_0(x,t_1)\exp(-t_1\sqrt{s_2D_\mathrm{h}}/R). \tag{A10}$$

The second inverse with respect to s_2, making use of Laplace transformation tables (Bronshtein et al., 2004, equation 62, p. 1064), results in

$$C(x,t_1,t_2) = C_0(x,t_1)\frac{t_1}{2R}\sqrt{\frac{D_\mathrm{h}}{\pi t_2^3}}\exp\left(-\frac{D_\mathrm{h}t_1^2}{4R^2t_2}\right). \tag{A11}$$

In view of Eqs. (A7) and (A8), Eq. (A11) yields the solution

$$C(x,t) = \int_0^t C_0(x,\tau)\frac{\tau}{2R}\sqrt{\frac{D_\mathrm{h}}{\pi(t-\tau)^3}}\exp\left[-\frac{D_\mathrm{h}\tau^2}{4R^2(t-\tau)}\right]\mathrm{d}\tau, \tag{A12}$$

as also given by Eq. (9) in the main text.

References

Bencala, K.E., 1984. Interactions of solute and streambed sediment, 2, a dynamic analysis of coupled hydrologic and chemical processes that determine solute transport. Water Resour. Res. 20 (12), 1804–1814.

Bencala, K.E., 2005. Hyporheic exchange flows. In: Anderson, M. (Ed.), Encyclopedia of Hydrological Sciences, vol. 3. Wiley, Ltd., New York, pp. 1733–1740, Pt. 10, Chap. 113.

Bencala, K.E., Walters, R.A., 1983. Simulation of solute transport in a mountain pool-and–riffle stream: a transient storage model. Water Resour. Res. 19 (3), 718–724.

Bencala, K.E., McKnight, D.M., Zellweger, G.W., 1990. Characterization of transport in an acidic and metal-rich mountain stream based on a lithium tracer injection and simulations of transient storage. Water Resour. Res. 26 (5), 989–1000.

Brevis, W., Vargas J., Debels P., Link O., 2001a. Efecto de las zonas de almacenamiento transitorio en la modelación de la demanda bioquímica de oxígeno: Aplicación al Rio Chillán, Chile, Anales de XV Congreso Chileno de Ingeniería Hydráulica, Sociedad Chilena de Ingeniería Hydráulica, Concepción, Chile, pp. 119–129
Brevis, W., Debels P., Vargas J., Link O., 2001b. Comparación de Métodos para estimar el coeficiente de dispersión longitudinal en el Río Chillán, Chile. Anales de XV Congreso Chileno de Ingeniería Hidráulica, Sociedad Chilena de Ingeniería Hidráulica, Concepción, Chile, pp. 155–164.
Bronshtein, I.N., Semendyayev, K.A., Musiol, G., Muehlig, H., 2004. Handbook of Mathematics, 4th ed. Springer, New York, 1153 p.
Chatwin, P.C., 1980. Dispersion in natural streams. J. Hydraul. Div., ASCE 97 (HY1), 71–83.
Choi, J., Harvey, J.W., Conklin, M.H., 2000. Characterizing multiple timescales of stream and storage zone interaction that affect solute fate and transport in streams. Water Resour. Res. 36 (6), 1511–1518.
Czernuszenko, W., Rowinski, P.M., 1997. Properties of the dead-zone model of longitudinal dispersion in rivers. J. Hydraulic Res. 35 (4), 491–504.
Czernuszenko, W., Rowinski, P.M., Sukhodolov, A., 1998. Experimental and numerical validation of the dead-zone model for longitudinal dispersion in rivers. J. Hydraulic Res. 36 (2), 269–280.
Davis, P.M., Atkinson, T.C., Wigley, T.M.L., 2000. Longitudinal dispersion in natural channels: 2. The roles of shear flow dispersion and dead zones in the River Severn, UK. Hydrol. Earth Syst. Sci. 4 (3), 355–371.
Day, T.J., 1975. Longitudinal dispersion in natural channels. Water Resour. Res. 11 (6), 909–918.
De Smedt, F., 2006. Analytical solutions for transport of decaying solutes in rivers with transient storage. J. Hydrol. 330, 672–680.
De Smedt, F., Brevis, W., Debels, P., 2005. Analytical solution for solute transport resulting from instantaneous injection in streams with transient storage. J. Hydrol. 315 (1–4), 25–39.
Fernald, A.G., Wigington Jr., P.J., Landers, D.H., 2001. Transient storage and hyporheic flow along the Willamette River, Oregon: field measurements and model estimates. Water Resour. Res. 37 (6), 1681–1694.
Fischer, H.B., List, E.J., Koh, R.C.Y., Imberger, J., Brooks, N.H., 1979. Mixing in Inland and Coastal Waters. Academic Press, London, 483 p.
Gooseff, M.N., Wondzell, S.M., Haggerty, R., Anderson, J., 2003. Comparing transient storage modelin and residence time distribution (RTD) analysis in geomorphically varied reaches in the Lookout Creek basin, Oregon, USA. Adv. Water Resour. 26 (9), 925–937.
Hart, D.R., 1995. Parameter estimation and stochastic interpretation of the transient storage model for solute transport in streams. Water Resour. Res. 31 (2), 323–328.
Harvey, J.W., Fuller, C.C., 1998. Effect of enhanced manganese oxidation in the hyporheic zone on basin-scale geochemical mass balance. Water Resour. Res. 34 (4), 623–636.
Harvey, J.W., Wagner, B.J., Bencala, K.E., 1996. Evaluating the reliability of the stream traces approach to characterize stream subsurface water exchange. Water Resour. Res. 32 (8), 2441–2451.
Hays, J.R., Krenkel, P.A., Schnelle, K.B., 1966. Mass transport mechanisms in open-channel flow, Technical Report No. 8, Department of Civil Engineering, Vanderbilt University, Nashville, Tennessee, 138 p.
Jackman, A.P., Walters, R.A., Kennedy, V.C., 1984. Transport and concentration controls for chloride, strontium, potassium and lead in Uvas Creek, a small cobble-bed stream in Santa Clara County, California, USA: 2. Mathematical modelling. J. Hydrol. 75, 111–141.
Keefe, S.H., Barber, L.B., Runkel, R.L., Ryan, J.N., McKnight, D.M., Wass, R.D., 2004. Conservative and reactive solute transport in constructed wetlands. Water Resour. Res. 40, W01201.
Laenen, A., Bencala, K.E., 2001. Transient storage assessments of dye – Tracer injections in rivers of the Willamette Basin, Oregon. J. Am. Water Res. Assoc. 37 (2), 367–377.
Lees, M.J., Camacho, L.A., Chapra, S.C., 2000. On the relationship of transient storage and aggregated dead zone models of longitudinal solute transport in streams. Water Resour. Res. 36 (1), 213–224.
Legrand-Marq, C., Laudelout, H., 1985. Longitudinal dispersion in a forest stream. J. Hydrol. 78, 317–324.
Liu, H., Cheng, H.D., 1980. Modified Fickian model for predicting dispersion. J. Hydraul. Div., ASCE 1 (HY6), 1021–1040.
Maloszewski, P., Zuber, A., 1990. Mathematical modelling of tracer behaviour in short-term experiments in fissured rocks. Water Resour. Res. 26 (7), 1517–1528.
Marquardt, D.W., 1963. An algorithm for least-squares estimation of non-linear parameters. SIAM 11, 431–441.
Morrice, J.A., Vallet, M.H., Dahm, C.N., Campana, M.E., 1997. Alluvial characteristics, groundwater–surface water exchange and hydrologic retention in headwater streams. Hydrol. Process. 11, 253–267.
Nordin, C.F., Troutman, B.M., 1980. Longitudinal dispersion in rivers: The persistence of skewness in observed data. Water Resour. Res. 16 (1), 123–128.
Runkel, R.L., 1996. Solution of the advective-diffusive equation: continuous load of finite duration. J. Environ. Eng. 122 (9), 830–832.
Runkel, R.L., 1998. One-dimensional transport with inflow and storage (OTIS): a solute transport model of streams and rivers. US Geol. Surv. Water Resour. Invest. Rep. 98-4018.
Runkel, R.L., Chapra, S.C., 1993. An efficient numerical solution of the transient storage equations for solute transport in small streams. Water Resour. Res. 29 (1), 211–215.
Runkel, R.L., McKnight, D.M., Rajaram, H., 2003. Modeling hyporheic zone processes. Adv. Water Res. 26 (9), 901–905.
Schmid, B.H., 1995. On the transient storage equations for longitudinal solute transport in open channels: temporal moments accounting for the effects of first-order decay. J. Hydraulic Res. 33 (5), 595–610.
Schmid, B.H., 2003. Temporal moments routing in rivers and streams with transient storage. Adv. Water Res. 26 (9), 1021–1027.
Sneddon, I.N., 1974. The Use of Integral Transforms. McGraw-Hill Publ. Co. Ltd., New York, 539 p.
van Mazijk, A., Veling, E.J.M., 2005. Tracer experiments in the Rhine Basin: evaluation of the skewness of observed concentration distributions. J. Hydrol. 307, 60–78.
Wörman, A., 1998. Analytical solution and timescale for transport of reacting solutes in rivers and streams. Water Resour. Res. 34 (10), 2703–2716.
Wörman, A., 2000. Comparison of models for transient storage of solutes in small streams. Water Resour. Res. 36 (2), 455–458.
Wörman, A., Packman, A.I., Johansson, H., Jonsson, K., 2002. Effects of flow-induced exchange in hyporheic zones on longitudinal transport of solutes in streams and rivers. Water Resour. Res. 38 (1), 2.1–2.15.